IOSR Journal of Applied Chemistry (IOSR-JAC)
e-ISSN: 2278-5736.Volume 9, Issue 1 Ver. I (Jan. 2016), PP 49-57
www.iosrjournals.org

Computational Study of p-Nitrobenzaldehydethiosemicarbazone: Synthesis and Biological Activity of its Cu^{II} and Hg^{II} Complexes

B. Sireesha[1]*, S. P. Mydhili[1], G. Sravan[1], CH. Venkataramana Reddy[2]
[1] *Department of Chemistry, Nizam College, O.U, Basheerbagh, Hyderabad, India.*
[2] *Department of Chemistry, College of Engineering JNTUH, Hyderabad, India.*

Abstract: *Computational energy calculations (semi-empirical and abinitio) were performed on geometrically optimized thione and thiol forms of the title compound. Minimum energy values, Heats of formation, dipole moments of the optimized geometries are evaluated, electrostatic potential, total spin density, total charge density maps and HOMO, LUMO surfaces are generated. Theoretical calculations are compared with the experimentally obtained data. Synthesized PNBTSC was characterized by LC-MS, IR, UV-Visible, ^1H NMR, ^{13}C NMR. Cu^{II} and Hg^{II} complexes of it were prepared and characterized by various spectro-analytical techniques like elemental analyses, molar conductance, magnetic susceptibility measurements, LC-MS, IR, UV-Vis, ^1H NMR, ESR, TGA and DSC. Elemental analyses and LC-MS studies reveal the composition of complexes as ML. The complexes showed good activity against gram positive and gram negative bacteria.*
Keywords: *antibacterial activity, bidentate nature, distorted octahedral geometry, semiemperical calculations, thermal analysis*

I. Introduction

Thiosemicarbazones are an important class of sulphur and nitrogen donor ligands for transition metal ions with good biological activity and medicinal properties such as antitumor, antifungal, anti bacterial, anti viral, anti cancer, anti inflammatory, anti malarial and anti-HIV [1-8] and other properties. Behnisch and his group reported thiosemicarbazones to be strongly tuberculostatic in vivo [9]. N. Raghav et al. studied the effect of semicarbazones, thiosemicarbazones, hydrazones and phenyl hydrazones of simple aryl aldehydes on the activity of liver alkaline phosphatase [10,11]. Antitrypanasomal activity of novel benzaldehyde thiosemicarbazone derivatives from Kaurenoic Acid were reported by Shirani K. Haraguchi et al [12]. Rama Acharyya and co workers studied Rhodium assisted C-H activation of benzaldehyde thiosemicarbazones and their oxidation via activation of molecular oxygen [13]. These compounds also have many applications in analytical, pharmaceutical, agricultural and industrial fields. The considerable research in the field of physiological activity of these compounds is due to their ability to chelate with traces of metal ions. The properties exhibited by these compounds were found to undergo significant changes on complexation.

The present communication reports computational energy calculations (semi-empirical and abinitio) on geometrically optimized thione and thiol forms of p-Nitrobenzaldehyde thiosemicarbazone (PNBTSC), synthesis of its binary metal complexes using MCl_2 [M= Cu^{II}, Hg^{II}], characterization using spectro analytical data and anti bacterial activity of the compounds.

II. Experimental

2.1. Materials and Methods

All the chemicals were of AR grade procured from Sigma-Aldrich. Semi-empirical AM1, PM3and abinitio quantum chemical calculations were carried out by the HyperChem^{TM} 7.5 Molecular Modeling program. Elemental analyses collected from Perkin-Elmer 240C elemental analyzer. The percentages of metal contents were determined by Atomic Absorption Spectrophotometer (AAS) on Perkin Elmer Scitex ELAN DRC ll by open acid digestion method. Molar conductivity was measured using Digisun digital conductivity meter model 909. LC-MS data of p-nitrobenzaldehyde thiosemicarbazone (PNBTSC) was collected on Shimadzu LCMS-2010A. Thermo gravimetric analyses of the complexes were carried on TGA Q50 V20.8 Build34 in the range 0°C-800°C and differential scanning calorimetric analysis of complexes was carried on DSC Q20 V24.2 Build107 system in the temperature range 0°C-500°C. IR spectra (KBR) were recorded on a Perkin –Elmer 435 Spectrophotometer. ^1H and ^{13}C-NMR spectra were recorded on Bruker WH (270MHz) spectrometer. UV spectra were scanned on EV100 UV-Visible spectrophotometer V 4.60. ESR spectra of oxovanadium, manganese and copper complexes were obtained from Jeol, JES–FA 200 ESR spectrometer. Magnetic susceptibilities were measured at room temperature on Faraday balance model 7550. Calibration constant was determined from standard $Hg[Co(SCN)_4]$.

2.2. Synthesis of PNBTSC

PNBTSC (Fig:1) was synthesized by dissolving equimolar solutions of thiosemicarbazide (0.01M) in hot water and p–nitrobenzaldehyde (0.01M) in 35 ml of methanol and refluxing the mixture for four hours. The yellow solid obtained was filtered and washed thoroughly with water. Purity of the compound was checked by TLC. Recrystallised from ethanol. M.P-210°C-212°C.

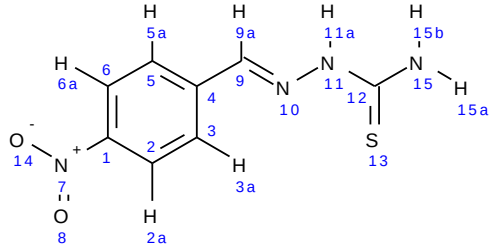

Fig 1: Structure of p-Nitrobenzaldehyde thiosemicarbazone

Elemental Analysis for $C_8H_8N_4O_2S$: Found (Calcd) %: C, 42.43(42.7); H, 3.82(3.85); N, 24.47(24.87); S, 14.50(14.24); IR (KBr, cm^{-1}): 3491 υ_{NH}; 3363 υ_{NH} (asymmetric and symmetric stretching of NH_2); 3286 υ_{NH}; 1589 $\upsilon_{C=N}$; 1000 υ_{N-N}; 819 $\upsilon_{C=S}$; ^{1}H NMR (DMSO-d_6, δ, ppm): δ 11.68 [s, 1H, N-N-**H]**; δ 8.43[(s, 1H, N-**H**]; 8.25 [s, 1H, N-**H**]; 8.13 [s, 1H, **H**-C=N]; 7.97-8.45 [m, 4H, aromatic-C-**H**]; ^{13}C NMR in DMSO-d_6 (δ, ppm): 178.5 (C_{12}); 147.5 (C_9); 140.7 (C_1); 139.6 (C_4); 128.1 (C_3,C_5); 123.7 (C_2,C_6). UV-Vis (DMSO, cm^{-1}): 26666 (n→ π* of thiosemicarbazone moiety); 36429 (π→ π* of thiosemicarbazone moiety); 38167 (π→ π* of nitro group, benzene ring); 47169 (π→ π* of benzene moiety); MS (APCI (+), (m/z):224.8$[M]^+$ ion peak.

2.3. Synthesis of metal complexes

To the hot ethanolic solution of the ligand, aqueous metal salt MCl_2 [M=Cu^{II}, Hg^{II}], solutions in 1:2 (M:L) molar ratio were added. Mixtures were refluxed for 6 to 8 hours. pH of the solutions were adjusted by the addition of few drops of ethanolic ammonium hydroxide solution. Solid complexes formed were filtered under hot condition, washed with hot methanol and water to remove unreacted ligand and metal salts respectively, then with petroleum ether and finally dried in vacuum [14].

2.4. Computational studies

Thione and thiol forms of PNBTSC were built, their geometry optimization is performed and the orbital energy diagrams are generated using Hyperchem 7.5. The total energy, heat of formation and dipole moment of the optimized geometries are calculated. Electrostatic potential, total spin, total charge densities were mapped. Highest occupied molecular orbital (HOMO), Lowest unoccupied molecular orbital (LUMO) have been generated. Important physical parameters like energies of HOMO and LUMO, their gap, hardness(η), ionisation potential(IP), and electron affinity(EA) that are important for studying chemical reactivity and biological properties are calculated [15,16]. Electrostatic potential mapping, reveal the reactive sites on the molecules [17,18]. Theoretically calculated UV and IR data have been compared with experimental results.

2.5. Biological Activity

Biological activity of all the complexes was tested using Kirby-Bauer disc diffusion method. 0.10ml of test bacteria [Staphylococcus aureus, Bacillus subtilis (gram positive), Escherichia coli, Klebsiella pneumonia (gram negative)] was spread over the surface of nutrient agar. Sterile discs of 5mm diameter dipped in DMSO solutions of test samples are placed at equidistance. The potency of all the samples tested was 1000 µg/disc. Capacity of the disc is 5µl of the sample. DMSO was taken as control which has no antibacterial activity. Gentamycin was used as standard. Zone of inhibition was recorded after incubation for 24hrs at 37°C. All these tests were run in triplicates and are averaged [1].

III. Results and Discussion

3.1. Computational Study of PNBTSC

To understand the stability and reactivity of PNBTSC, semi-empirical (AM1& PM3) and abinitio studies have been carried out. Thione and thiol forms of PNBTSC were built, preoptimized with molecular mechanics (AMBER) and then optimized more accurately with AM1 and PM3 semiemperical calculations. Single point energy, heat of formation and dipole moment of the optimized geometries were calculated using quantum mechanics and are presented in Table 1.

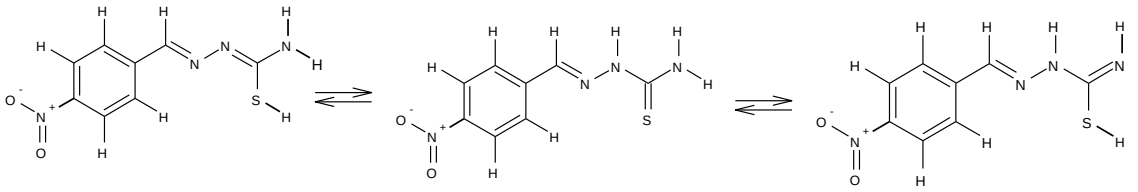

Thiol -1 Thione Thiol -2

Fig 2: Tautomers of PNBTSC

Table: 1 Molecular Properties of PNBTSC

Molecular Properties	Thione		Thiol -1		Thiol -2	
	AM1	PM3	AM1	PM3	AM1	PM3
Single Point Energy (kcal/mol)	-2304.44	-2258.56	-2302.39	-2323.22	-2293.92	-2264.99
Heat of formation (kcal/mol)	117.00	105.24	119.05	98.22	127.53	153.36
Dipole Moment (Debye)	10.77	11.64	9.79	10.59	6.82	8.25

The lower energies indicate that both thione and thiol forms of the compound are stable. Close proximity in energies of thione and thiol forms indicate the possibility of co-existence of both the forms. Calculated dipole moment values indicate more polar nature.

3.1.1. FMO Analysis

Analysis of HOMO and LUMO of the chemical compounds play an important role in understanding its chemical reactivity. Ionization energy (IE), electron affinity (EA) and hardness can be expressed as $-E_{HOMO}$, $-E_{LUMO}$ and 1/2 (E_{HOMO}- E_{LUMO}) respectively [15,16] and are shown in Table 2. A system with large gap between HOMO and LUMO will be less reactive and is harder in nature. In the present study, this gap is between 3.8 to7.54 ev indicating stability and hardness of the molecule in all the three forms also supported by their ionization energy.

Table: 2 Comparison of HOMO–LUMO energy, hardness, ionization energy, electron affinity

Energies	Thione		Thiol -1		Thiol -2	
	AM1	PM3	AM1	PM3	AM1	PM3
E_{HOMO} (ev)	-8.573	-6.564	-9.211	-9.137	-9.508	-7.514
E_{LUMO} (ev)	-1.803	-2.756	-1.671	-1.686	-1.744	-3.482
E_{HOMO}- E_{LUMO} (ev)	6.77	3.808	7.54	7.451	7.764	4.032
Hardness=1/2 (E_{HOMO}- E_{LUMO})	3.385	1.904	3.77	3.725	3.882	2.016
I.E=- E_{HOMO}	8.573	6.564	9.211	9.137	9.137	7.514
EA=- E_{LUMO}	1.803	2.756	1.671	1.686	1.744	3.482

The optimized structures of thione-thiol forms, electrostatic potential, electron density mappings and the generated molecular orbital energy diagrams - HOMO, LUMO in AM1and PM3 methods are presented in Fig:3. Electrostatic potential mapping gives information about the reactivity of the molecule with nucleophilic/electrophilic reagents. From the electrostatic potential mapping violet region around oxygen and nitrogen atoms with imine linkages indicate negative ESP, hence more susceptible to electrophilic attack by a suitable molecule.

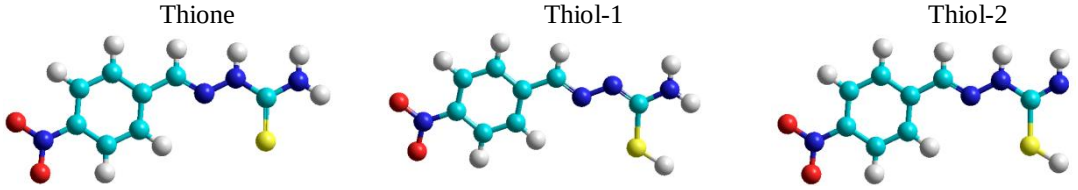

3(a): Optimized geometry

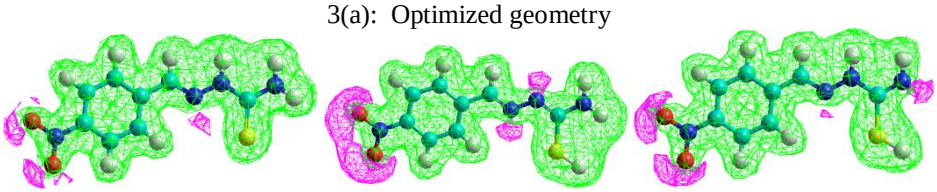

3(b): Electrostatic Potential

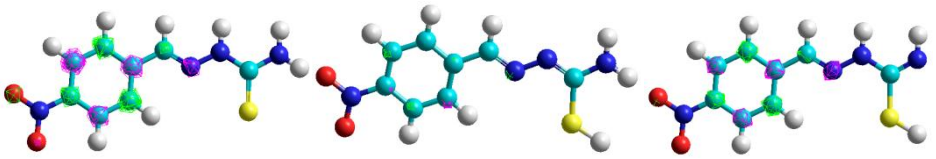

3(c): Total Spin Density

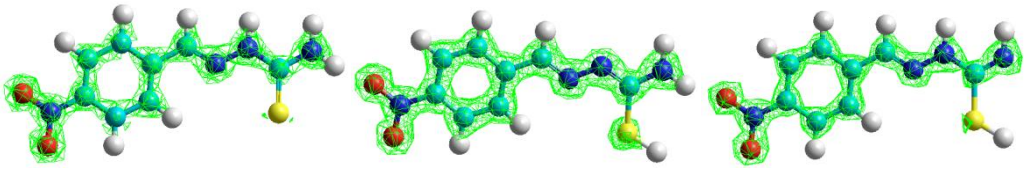

3(d): Total Charge Density

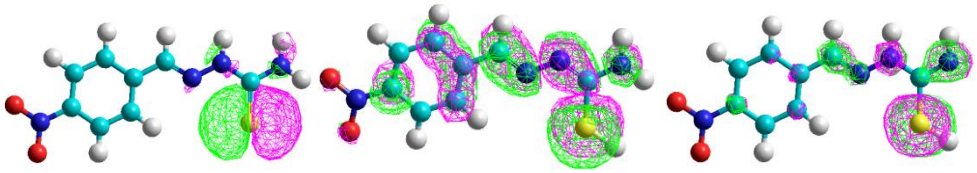

3(e): Highest occupied molecular orbitals

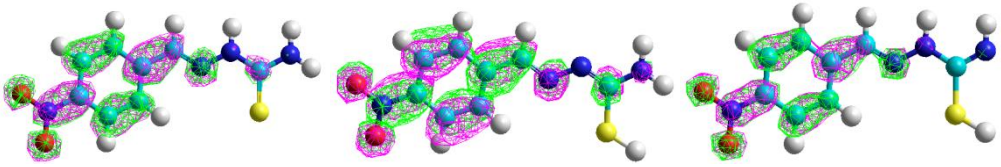

3(f): Lowest unoccupied molecular orbitals

Fig 3(a-f): Molecular graphs of PNBTSC

3.1.2. QSAR Studies

QSAR studies helps to recognize and compute the physico chemical properties of a drug and its effect on biological activity. The most common physico chemical properties include hydrophilic, electronic and steric nature. Hydrophobic character of a drug is crucial in identifying its ease in crossing the cell membrane and its interaction with the receptor. It is measured in terms of partition coefficient.

Partition coefficient = Conc. of drug in octanol / Conc. of drug in aqueous solution (1)

By plotting log p vs log 1/concentration, it is possible to correlate drug with biological activity. In general, drugs with log p nearly 3.0 have greater chance of being absorbed, higher than 4.0 require lipid formulations and less than 2.0 shows both hydrophilic and hydrophobic character and are difficult to formulate. From log p values of the ligand (Table: 3) in thione and thiol forms it can be understood that ligand possess good penetrating capability into cell membrane and inturn has considerable biological activity [19].

Table: 3 QSAR Properties

Properties(Abinitio)	Thione	Thiol -1	Thiol -2
Partial charge	0.00e	0.00e	0.00e
Surface area (approx) (A^{02})	383.03	404.45	384.63
Surface area (grid) (A^{02})	414.34	417.97	415.78
Volume (A^{03})	641.04	645.16	642.33
Hydration energy (K.cal/mol)	-20.20	-21.67	-18.53
Log P	2.35	2.64	2.81
Refractivity (A^{03})	61.69	60.34	60.22
Polarizability (A^{03})	22.83	22.16	22.16
Mass (amu)	224.24	224.24	224.24

3.1.3. Comparison of theoretical calculations with experimental data

Theoretically obtained UV and IR data using AM1 and PM3 methods have been compared with experimental data in Tables 4 and 5. Vibrational frequencies of three forms of the Schiff base were calculated. Some vibrations found in the experimental spectra (solid phase) of thione form could not be identified in the simulated equivalent and therefore, have been omitted. This may be due to anharmonicity, intermolecular interaction, an approximation treatment of electron correlation effects and the limited basis sets. The correlation coefficient (cc) values for AM1 and PM3 semi-empirical methods are 0.982 and 0.994 respectively for thione form of PNBTSC. It is apparent from these values that PM3 semi-empirical method gives more satisfactory correlation between experimental and calculated vibrational frequencies.

Table: 4 Comparison of UV data

Assignment	Thione			Thiol-1		Thiol-2	
	Exp	AM1	PM3	AM1	PM3	AM1	PM3
π→ π*	212.5	204.21	224.67	212.95	215.29	213.86	216.4
π→ π*	262.0	259.19	249.69	275.47	295.53	281.81	283.31
π→ π*	274.5	324.44	283.28	286.19	318.11	292.03	298.43
n→ π*	375.0		353.45				

Table: 5 Comparison of IR data

Assignment		Thione		Thiol-1		Thiol-2
Stretching vibration	Exp	AM1	PM3	AM1	PM3	AM1
υ N-H (thioamide)	3363	3354	3297	3344	3328	3436
υ N-H(imine)	3286	3443	3144	----	----	3436
υ C-H aromatic	3092-2804	3323	3188	3327,3319	3187,3178	3331
υ C=N	1589	1946	1709	1946,1860	1868,1759	1952,1886
υ N-O	1525	1579	1413	1513	1402	1567
υ Ar C=C	1514,1450	1726,1339	1688	1726,1587	1717,1501	1725,1520
υ N-N	1000	1458	1048	1446	1076	1418
υ C=S	819	766	769	----	----	---
υ S-H	----	----	----	1967	1569	1960
υ C-S	----	----	----	626	600	660

Reasonable deviations of calculated values from experimental values is due to the fact that theoretical calculations have been actually performed on single molecule in gaseous state contrary to the experimental values recorded in the presence of intermolecular interactions.

3.2. Characterization of complexes

All the complexes synthesized are coloured, amorphous, stable to air and moisture, soluble in DMSO and DMF. Elemental analyses data revealed the formation of 1:1 (M:L) ratio. Presence of chloride in complexes was identified from Volhard's test [20]. Physical properties of PNBTSC and its complexes are given in Table 6. Molar conductivity measurements were recorded in 1x10-3M DMSO solutions at room temperature. Low values (5 to 15 $ohm^{-1}cm^2$ mol^{-1}) indicate that the complexes are nonelectrolytes.

Table: 6 Physical and Analytical Data of PNBTSC and its Metal Complexes

Compound	Colour	M.P (°C)	%C Obs (Calcd)	%H Obs (Calcd)	%N Obs (Calcd)	%S Obs (Calcd)	%M Obs (Calcd)	Conductivity ($\Omega^{-1}cm^2mol^{-1}$)
PNBTSC	Shiny Cream	210 - 212	42.43 (42.70)	3.82 (3.85)	24.47 (24.87)	14.50 (14.24)	----	----
[$CuCl_2$(PNBTSC)(H_2O)$_2$]	Reddish Brown	Dp	24.13 (24.32)	3.12 (3.04)	14.41 (14.18)	8.11 (8.11)	16.14 (16.09)	015
[HgCl(PNBTSC)(H_2O)$_3$]	Light Cream	Dp	19.03 (18.70)	2.46 (2.53)	10.74 (10.90)	6.44 (6.23)	----	005

3.2.1. Liquid chromatograms

Both the complexes showed single peak with retention time 0.551min indicating their purity.

3.2.2. Mass Spectra

ESI(+) spectrum of Cu^{II}-PNBTSC(Fig:4a) showed molecular ion peak at m/z 395.5. A peak at m/z 288 is due to loss of two coordinated water molecules and two chloride ions. Peak at m/z 64 indicates metal ion with loss of $[PNBTSC]^+$ ion. Peak at m/z 512 in ESI(+) spectrum of Hg^{II}-PNBTSC(Fig:4b) correspond to its $[M+1]^+$ ion. Peak at 460 is due to loss of three water molecules. Peaks at m/z 246 and m/z 224 indicate $[PNBTSC+Na]^+$ and $[PNBTSC-H]^+$ respectively.

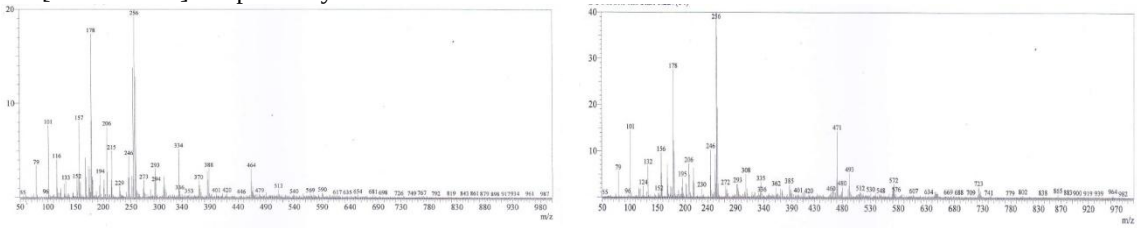

4(a): Cu^{II}-PNBTSC 4(b): Hg^{II}-PNBTSC

Fig 4(a&b): Mass spectra of complexes

3.2.3. Thermal Analysis

Themo Gravimetric Analyses for the complexes were recorded at 0°C-800°C and Differential Scanning Calorimetric analyses at 0°C -500°C. TGA of Cu^{II}-PNBTSC (Fig:5a) showed weight loss in four steps. Decomposition of 245°C -260°C (3%) indicates the loss of coordinated water molecules from the complex. Gradual weight loss in the range of 260°C-800°C is attributed to the decomposition of the ligand moiety. Residue (42.5%) corresponds approximately to CuO.

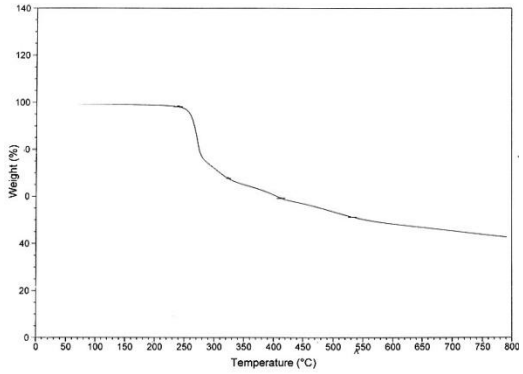

5(a): Cu^{II}-PNBTSC

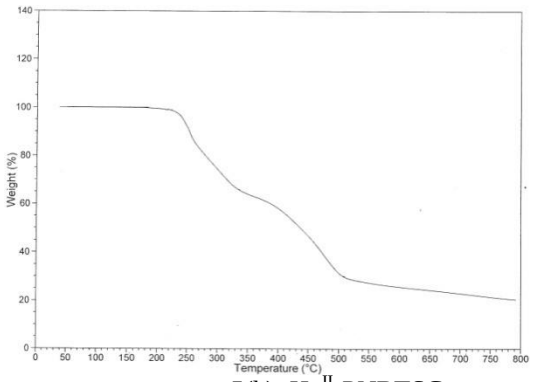

5(b): Hg^{II}-PNBTSC

Fig 5(a&b): Thermograms of Complexes

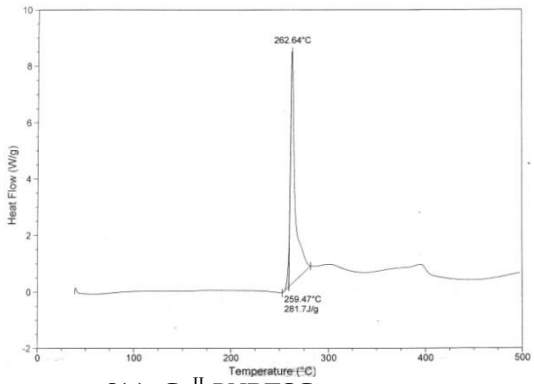

6(a): Cu^{II}-PNBTSC

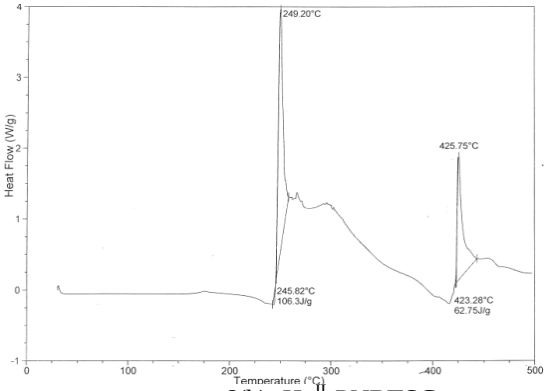

6(b): Hg^{II}-PNBTSC

Fig 6(a&b): Differential Scanning Calorimetry of Complexes

Thermogram of Hg^{II}-PNBTSC (Fig:5b) showed the weight loss in three steps. Weight loss in the temperature range of 200-250°C (7%) indicates the loss of three coordinated water molecules from the complex. The maximum weight loss in the range of 300°C-500°C in two steps is attributed to the stepwise decomposition of ligand and sudden weight loss till 800°C (10%) indicate decomposition of both ligand and metal moieties. The percentage residue left at 800°C for Cu^{II}- PNBTSC and Hg^{II}-PNBTSC complexes approximately coincides with the metal content expected from 1:1 composition of the complexes. DSC curves of the complexes (Fig 6a & 6b) showed exothermic peaks indicating various chemical changes occurring in the complexes accompanied by the energy release.

3.2.4. IR Spectra

IR spectral data is useful to identify the potential donor sites of the ligand during complexation with the metal ions. IR spectra of Cu^{II} and Hg^{II} complexes of PNBTSC **(**Fig 7(a&b)) showed a broad trough ranging from $\upsilon 3500 cm^{-1}$-$\upsilon 3100 cm^{-1}$ is attributed to coordinated water molecules in the complexes. This is also supported from TGA studies discussed earlier. The (C=N) stretching frequency of thiosemicarbazone moiety in PNBTSC observed at $\upsilon 1589\ cm^{-1}$ is shifted to $\upsilon 1585\ cm^{-1}$ in IR spectrum of Cu^{II}-PNBTSC (Fig: 7a). This indicates coordination of azomethine nitrogen, supported by an increase in N-N stretching frequency. Shift of C=S band from $\upsilon 819\ cm^{-1}$ of the ligand to $\upsilon 813\ cm^{-1}$ suggest complexation of thione sulphur with Cu^{II} metal ion. Thus PNBTSC acts as a bidentate ligand binding to metal with azomethine nitrogen and thione sulphur, forming five membered chelate.

A broad N-H (imine) band centered at $\upsilon 3286 cm^{-1}$ in the ligand is lost in IR spectrum of Hg^{II}- PNBTSC (Fig: 7b) and a new C=N at $\upsilon 1616 cm^{-1}$ is observed along with $\upsilon 1581 cm^{-1}$. This shows loss of N-H proton via thione-thiol tautomerism in this complex. The decrease in C=N stretching from $\upsilon 1589\ cm^{-1}$ to $\upsilon 1581 cm^{-1}$

indicating coordination of azomethine nitrogen, supported by an increase in N-N stretching frequency. The shift in the frequency due to C=S of the ligand from υ819cm^{-1}to υ806cm^{-1} attributed to bond formation between sulphur and Hg^{II} ion.

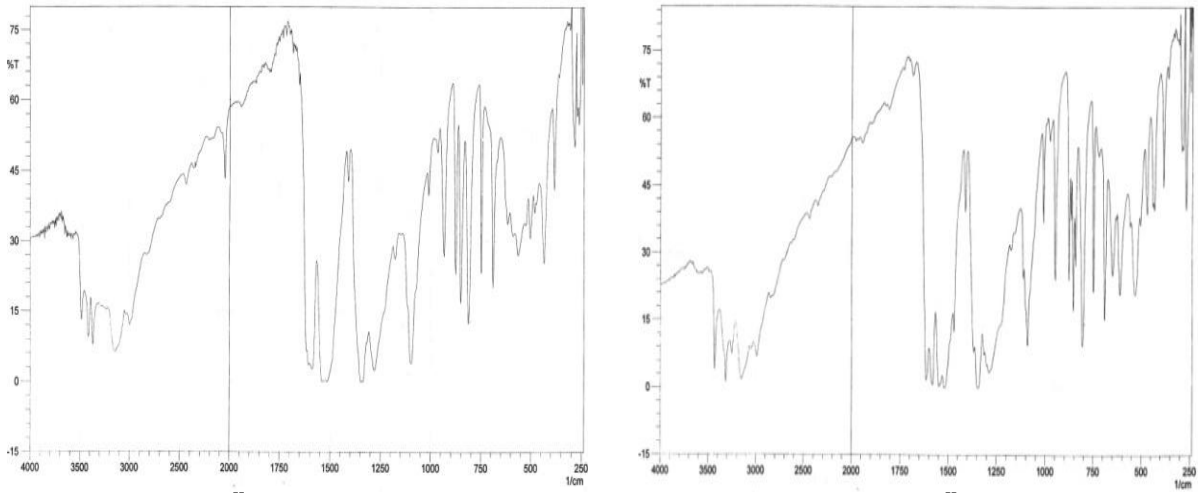

7(a): Cu^{II}-PNBTSC 7(b): Hg^{II}-PNBTSC

Fig 7(a&b): IR spectra of Complexes

From the Far IR region of the spectra there is evidence for the presence of M-N (υ478cm^{-1} to υ482cm^{-1}), M-Cl (υ315cm^{-1} to υ318cm^{-1}), M-OH_2 (υ440cm^{-1}) bonds in the complexes. Comparative analyses of IR spectral data shows that the ligand is bidentate in nature with azomethine nitrogen and thione/thiolate sulphur as potential donor sites and can form five membered chelates with both the metals.

3.2.5. ^{1}H NMR spectrum

Peak at δ 11.68ppm that belongs to hydrazine proton in the spectrum of PNBTSC (Fig :8a) is absent in ^{1}H NMR spectrum of Hg^{II}-PNBTSC (Fig :8b). The characteristic signal of thiol proton at 4ppm [4] is also absent revealing the coordination of thiolate sulphur to Hg^{II} ion.

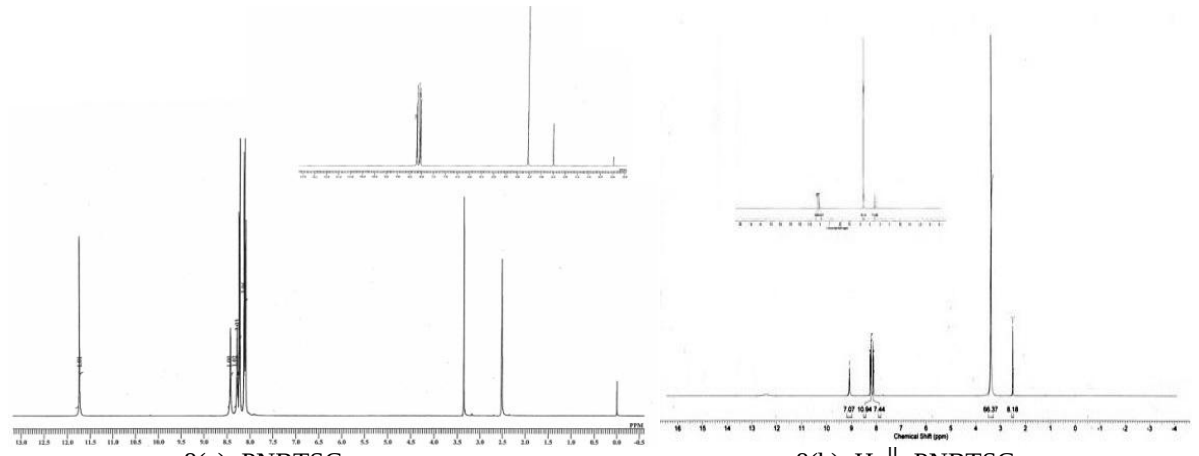

8(a): PNBTSC 8(b): Hg^{II}- PNBTSC

Fig 8(a&b): ^{1}HNMR spectra of PNBTSC and Hg^{II}- PNBTSC (Inset: D_2O exchange Spectra)

3.2.6. UV-Vis spectrum

In addition to the ligand chromophores, UV-Visible spectrum of Cu^{II}-PNBTSC shows a broad shoulder like peak at 22,222cm^{-1} that can be assigned to $^2E_g \rightarrow {}^2T_2g$ transition expected for d^9 configuration with distorted octahedral geometry.

3.2.7. ESR spectrum

The ESR spectrum of Cu^{II}-PNBTSC in DMSO showed well resolved peaks at g∥ 2.23 and g$^{\perp}$ 2.16, 2.09, 2.02. The greater values of g∥ suggest distortion from regular octahedral geometry and anisotropic environment around copper ion. The g∥ <2.3 indicate covalent nature of Cu-L bond. Both g∥ and g $^{\perp}$ >2.0023

signify the presence of unpaired electron in d_{x2-y2} orbital of the Cu^{II} ion. Axial symmetry parameter G<4 was due to exchange interaction between metal centers of polycrystalline compound [21].

3.2.8. Magnetic Susceptibility Measurements

The Cu^{II}-PNBTSC possesses a magnetic moments 1.64 B.M. corresponding to one unpaired electron indicating the distorted octahedral geometry.

From the investigations of spectro-analytical data, the structures for the metal complexes of PNBTSC are tentatively predicted (Fig: 9a&b).

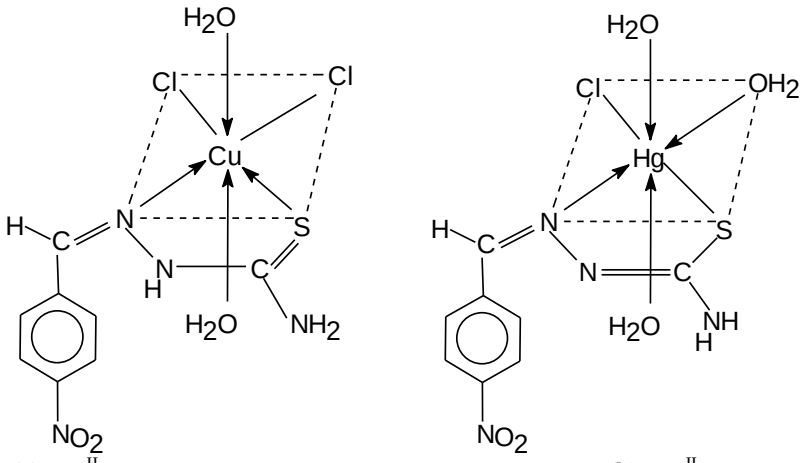

9(a): Cu^{II}-PNBTSC 9(b): Hg^{II}-PNBTSC

Fig 9 (a&b): Proposed structures of complexes

3.3. Biological Activity

Activity of PNBTSC and its complexes have been tested on both gram positive and gram negative bacteria. The ligand PNBTSC does not possess antibacterial activity. Cu^{II}-PNBTSC is active against Staphylococcus, Bacillus and Klebsiella where as Hg^{II}- PNBTSC is found to inhibit the growth of all the bacteria under study. This can be attributed to the chelating capacity of the metal to ligand. Metal atom partially shares its positive charge with the donor atoms of the ligand. This leads to delocalization of π electron cloud over the chelating ring. Due to this the lipophilic character of the metal gets enhanced and favours its permeability into bacterial cell membranes and inhibits the growth of the bacteria. The zone of inhibition of the ligand and its complexes is given Table 7.

Table: 7 Anti Bacterial Activity of ligand and complexes

S.No	Staphylococcus	E. coli	Bacillus	Klebsiella
PNBTSC	----	----	----	----
Cu^{II}- PNBTSC	8 mm	----	12 mm	6 mm
Hg^{II}- PNBTSC	12 mm	8 mm	15 mm	10 mm

IV. Conclusion

Energy parameters from computational calculations show possible coexistence of thione and thiol forms. In Electrostatic potential, total spin and total charge density maps, nitrogen atoms with imine linkages indicate negative ESP, hence more susceptible to electrophilic attack by a suitable agent. Energy gap between HOMO and LUMO proved stability and hardness of the molecule. Comparison of theoretical IR spectral data with experimental data showed that PM3 semi-empirical calculations give more acceptable correlation. QSAR properties generated show good penetrating capacity of the ligand into cell membrane. Spectral characterization indicate that PNBTSC is a bidentate ligand forming distorted octahedral complexes with copper(II) and mercury(II) ions in 1:1 (M:L) composition. Both the complexes show good antibacterial activity against gram positive and gram negative bacteria with a promising future of these complexes in medicinal field.

Acknowledgements

The authors thank School of Chemistry and CIL, University of Hyderabad for providing ESR spectra, Dept. of Microbiology, UCS, Osmania University for antibacterial studies.

References

[1] S. Chandra, M. Tyagi and M. S Refat, Journal of Serbian Chemical Society, 74 (8-9)**,** 2009, 907-915.
[2] A. R. Cowley, J.R. Dilworth and P.S. Donnelly, John Woollard-Shore, Dalton Transactions, 2003, 748 -754.
[3] I. C. Mendes, L. R.Teixeira, R. Lima, H. Beraldo, N. L. Speziali and D. X. West, Journal of Molecular Structure, 559, 2001, 355-360.
[4] S. A. Elsayed, A. M. El-Hendaway, S. I. Mostafa and I. S. Butler, Inorganica Chimica Acta, 363, 2010, 2526-2532.
[5] J. Wiecek, D. Kovala-Demertzi, Z. Ciunik, J. Wietrzyk, M. Zervou and M. A Demertzis, Bioinorganic Chemistry and Applications, 2010, Article ID 718606 7.
[6] P. F. Raphel, E. Manoj and M. R. Prathapachandra Kurup, Polyhedron, 26, 2007, 818-828.
[7] E. N. Nfor, S. N. Esemu, G. A. Ayimele, E. A. Eno, G. E. Iniama and O.E. Offiong, Bulletin of the Chemical Society of Ethiopia, 25(3), 2011, 361-370.
[8] D. G. Calatayud, E. Lopez-Torres, M. Mendiola and J. R. Procopio, Zeitschrift für anorganische und allgemeine Chemie, 633, 2007, 1925-1931.
[9] R.Behnish, F. Mietzsch, H, Schmidt, Neue schwefelhaltige; Chemotherapeutika. Angew. Chem. 60A,1 948, 113-115.
[10] N. Raghav, M. Singh, S. Jangra, A. Rohilla, R. Kaur and P. Malik, Journal of Chemical and Pharmaceutical Research, 2(4), 2010, 801-807.
[11] N. Raghav, M. Suman, A. Ravinder and Priyanka; International Journal of Applied Biology and Pharmaceutical Technology, 1(3), 2010, 1011-1015.
[12] S. K. Haraguchi , A. A. Silva , G. J. Vidotti , P. V. dos Santos, F. P. Garcia , R. B. Pedroso , C. V. Nakamura , C. M. A. de Oliveira and C. C. da Silva , Molecules, 16, 2011, 1166-1180.
[13] R. Acharyya, S. Dutta, F. Basuli, Shie-Ming Peng, Gene-Hsiang Lee, L.R. Falvello and S. Bhattacharya D, Inorganic Chemistry, 45(3), 2006, 1252-1259.
[14] B.Sireesha, G. Bhargavi, C. Sita and Ch. Sarala Devi, Bulletin of pure and applied sciences 25C (1), 2006, 1-6.
[15] S. Rajeev, D. Kumar, S. Bhoop, V.K. Singh and R. Sharma, Research Journal of Chemical Sciences, 3(2), 2013, 79-84.
[16] R.Singh, D. Kumar, Y.C. GOswami and R.Sharma, Arabian Journal of Chemistry, 2014, DOI:10.10ma 16/j.arabjc.2014.10.022.
[17] S. J. Smith and B. T. Sutcliffe, Reviews in Computational Chemistry, 70, 1997, 271–316.
[18] C.J. Cramer, Essentials of Computational Chemistry: Theories and Models (NJ: John Wiley & Sons, 2002).
[19] Graham Patrick, An Introduction to Medicinal Chemistry (5th edition, Oxford University Press, 2013).
[20] A.I. Vogel , A Text Book Of Quantitative Inorganic Analysis (3rd edition, Longman, 1968)
[21] B. Anupama, CH.V.R. Reddy, C.G. Kumari, Chemical Science Transactions, 2(2), 2013, 461-466.